CERN - EUROPEAN ORGANIZATION FOR NUCLEAR RESEARCH

Submitted to
Nuclear Physics B

CERN/EP/PHYS 76-41
30 June 1976

PRISM PLOT ANALYSIS OF THE REACTION $\pi^- p \to p\pi^+\pi^-\pi^-$ AT 16 GeV/c

Aachen-Berlin-Bonn-CERN-Cracow-Heidelberg-Warsaw Collaboration

H. GRÄSSLER, R. HONECKER and H.G. KIRK
III. Physikalisches Institut der Technischen Hochschule, Aachen.

J. KLUGOW and R. NAHNHAUER
Institut für Hochenergiephysik der Akademie der Wissenschaften der DDR, Berlin-Zeuthen.

R. HARTMANN and G. ZOBERNIG
Physikalisches Institut der Universität Bonn.

P. KOSTKA*, D.R.O. MORRISON and F.A. TRIANTIS
CERN, European Organization for Nuclear Research, Geneva.

W. DORTH, M. HEIDEN, J. STIEWE and J. WOTSCHACK
Institut für Hochenergiephysik, Heidelberg.

(*) Now at Inst. für Hochenergiephysik der Akad. der Wissensch., Berlin-Zeuthen.

VTC/mk

CERN/EP/PHYS 76-41

ABSTRACT

A Prism Plot Analysis of the reaction $\pi^- p \to p\pi^+\pi^-\pi^-$ at 16 GeV/c has been made and the results are compared with those obtained in a similar analysis of the reaction $\pi^+ p \to p\pi^+\pi^+\pi^-$ at the same energy. The three dominating reaction mechanisms - pion dissociation, Reggeon exchange, proton diffraction dissociation - appear to be well separated, while considerable residual overlaps are present inside these classes. The Prism Plot Method is discussed as a means for detecting hidden structures and some evidence is presented for a broad three-pion enhancement around 2 GeV decaying primarily into $\rho^o\pi^-$.

CERN/EP/PHYS 76-41

1. INTRODUCTION

In this paper we report on the reaction:

$$\pi^- p \rightarrow p\pi^+\pi^-\pi^- \qquad (1)$$

at 16 GeV/c incident pion momentum, measured in an experiment using the CERN 2m H_2 bubble chamber. The Prism Plot Analysis (PPA) of reaction (1) is an extension of our work on the reaction:

$$\pi^+ p \rightarrow p\pi^+\pi^+\pi^- \qquad (2)$$

at the same energy, the results of which have been published in ref. [1].

The PPA, proposed by Pless and co-workers [2], is an approach to obtain a separation of reaction subchannels contributing to a given final state, superior to that achieved by "conventional" methods (e.g., maximum likelihood fitting, LPS analyses).

A detailed survey of how the method works was given in ref. [3], while the special application to reaction (2) is sketched in ref. [1], where a summary is given of terminology, choice of variables, advantages and shortcomings of the PPA in its present stage. Since reaction (1) has the same kind and number of final state particles and the same number of identical particles as reaction (2), the technical apparatus used to perform a PPA of reaction (2) can be applied almost unchanged to reaction (1). Therefore, we do not repeat technical details previously presented.

2. CONTRIBUTING CHANNELS

Reaction (2) has been found to be dominated by three main classes of reaction mechanisms: (i) pion diffraction dissociation, (ii) double resonance production, and (iii) proton diffraction dissociation. It is therefore natural to begin a PPA of reaction (1) by introducing the same reaction channels as in (2) after performing the necessary isospin rotations: A_1^+ p replaced by A_1^- p, $\Delta^{++}\rho^o$ by $\Delta^o\rho^o$, etc.

One is certainly justified in expecting a strong similarity in the properties of diffraction-like processes for π^+ and π^- projectiles, e.g. $\pi^\pm p \to A_1^\pm p$, $\pi^\pm p \to \pi^\pm(p\pi^+\pi^-)$, because the mechanism of excitation of projectile or target is supposed to be independent of the charge of the exciting particle. For processes where isospin is exchanged the situation is less simple, but as a first guess the introduction of the (isospin rotated) channels separated in reaction (2) seemed reasonable.

Summarizing the results: We found copious production of A_1^-, A_2^- and A_3^- and evidence for the negative A'(1800), a broad (3π) enhancement peaking near 1800 MeV, the existence of the positive A' having been reported in ref. [1]. Furthermore, after a few iteration steps, it became clear that proton diffraction dissociation could be established with properties similar to those observed in reaction (2).

Quite a different behaviour was found in the reactions of the "double resonance production" type, which in reaction (2) was governed by $\Delta^{++}\rho^o$ production, followed in importance by Δ^{++} f and $\Delta^{++}g^o$ production. Looking for the corresponding channels in reaction (1) we found it impossible to obtain a stable contribution of $\Delta^o\rho^o$, to say nothing of Δ^o f and $\Delta^o g^o$. Also no indication was found for the production of a high mass Δ^o state, Δ^o(1900), together with a ρ^o. Assuming double resonance processes to be dominated by pion exchange, we expect the production of $\Delta^o\rho^o$ suppressed by a factor of 1/9 with respect to the production of $\Delta^{++}\rho^o$ in reaction (2). The number of events expected for $\Delta^o\rho^o$ is only 80, corresponding to 1.5% of the cross section for reaction (1). This fact leaves us with the impossibility of performing an unambiguous analysis of this channel. We therefore decided to open new channels for the production of a ρ^o and f recoiling off a low mass ($p\pi^-$)-system covering Δ^o(1236) as well as higher and non-resonant states. We did not try to add a channel containing the g^o. Finally, we had to introduce a channel for Δ^{++}(1236) production associated with a pair of uncorrelated negative pions. As a result, we were left with 9 sub-channels contributing to reaction (1). The channels are listed in table 1.

3. PARAMETRIZATION OF THE MONTE-CARLO DISTRIBUTIONS

The PPA is an iterative comparison between the experimental data and a set of Monte-Carlo-generated channels, the kinematic properties of which are taken from the previous step of the iteration. While all angular distributions are allowed to float freely during the course of iterations until convergence is obtained, the mass distributions of the well known resonances (Δ(1236), ρ, f and A_2) are parametrized as Breit-Wigner functions. The mass shape of the A_1 was taken from the Partial Wave Analysis reported in ref. [4]. The mass distributions of the A_3, A' and proton diffraction dissociation channels were allowed to float. The parametrization of the starting parameters was the same as in ref. [1], but experience showed that the choice of the initial shape has nearly no influence on the development of the iteration process.

4. RESULTS

The present analysis of reaction (1) is based on a total of 5190 events corresponding to a cross section of 1.13 mb. As said in sect. 3, this is only 20% of the events available for the PPA of reaction (2) reported in ref. [1], so a detailed comparison of the results is hindered by the poorer statistics.

The PPA - iteration process became stable after performing 32 steps. Summing up the final weights for the 9 sub-channels under consideration, we obtained the event numbers presented in table 1. There is, however, the question of how successful the separation has been, or, in other words, how strong the residual overlaps in phase-space still are. This is answered by the overlap matrix OV_{ij} presented in table 2 which gives the percent overlap between channels i and j with respect to channel i. For the definition of OV_{ij} see ref. [1]. The dotted lines indicate regions of "related" channels which are supposed to proceed via equal, or at least similar, mechanisms and consequently occupy the same or neighbouring regions in phase-space. As expected, we find the strongest overlaps between channels due to the same class of reaction mechanism. There are, however, also considerable overlaps between some of the non-related channels; most of the overlaps between two channels from different classes are, however, well below ten percent, which we consider to be a satisfying separation.

One of the conclusions drawn from the overlap information is that the PPA is unable to yield reliable cross sections for reaction channels which proceed via the same, or similar, dynamical processes and therefore occupy the same or neighbouring phase-space regions. This is in particular the case for the A meson sample and the proton diffraction dissociation sample, and has already been observed in the analysis of reaction (2). On the other hand, the separation of the three different classes of reaction mechanisms - pion diffraction dissociation (channels 1-4), Reggeon exchange (channels 5-7) and proton diffraction dissociation (channels 8 and 9) - is quite satisfactory and in good agreement with the results obtained analyzing reaction (2). To demonstrate this, we have calculated a 3 x 3 overlap matrix combining channels 1-4, 5-7, and 8-9, respectively (see table 3). Overlaps between different classes are indeed small so that we can trust the cross sections for these combined channels.

Cross sections for $\pi^- p$ and $\pi^+ p$ reactions are compared in table 4. We find good agreement not only for the sum of all A meson cross sections, but also for the sum of those A mesons decaying into $\rho^o \pi^-$.

The agreement between the proton diffraction dissociation samples in $\pi^+ p$ and $\pi^- p$ interactions is less satisfactory, but acceptable within the errors. There is no possibility for a direct comparison between the double resonance (or Reggeon exchange) samples.

In fig. 1 we present the invariant mass distributions for the original unseparated data. Although the separation is incomplete as the overlaps between different contributing channels are considerable, we present here in figs 2-10 mass, momentum transfer and decay angular distributions for the nine reaction channels considered. These distributions exhibit certain characteristic features already observed in the analysis of reaction (2) which - as far as they are comparable - show that some dynamical properties are revealed despite the obscuring influence of phase space overlaps. This is in particular the case for the A' sample: While the A'^- mass signal is less convincing and somewhat different in shape from the A'^+, the decay angular distributions shown in fig. 4 exhibit exactly the same behaviour as observed for the A'^+ sample in reaction (2).

Double resonance production as previously mentioned can less clearly be observed in this reaction than in reaction (2). In the invariant mass spectrum of the $(p\pi^-)$ system recoiling off the ρ^o (channel 5) we find in fig. 5 an indication of $\Delta^o(1236)$ plus an enhancement that might be due to the production of some higher mass isobars. The ρ^o signal itself appears to be clean. Also a small signal for f production together with a low mass $(p\pi^-)$ enhancement can be separated; in the $(\pi^+\pi^-)$ mass spectrum for the f decay, there appears in fig. 6 a weak g^o signal at the high mass shoulder of the f.

The total number of events not attributed to any of the channels introduced ("untagged" events) is 156, i.e. 3% of the total. None of the mass distributions for these events shows any structure (fig. 10); therefore we conclude that no important channel contributing to reaction (1) has been overlooked.

5. CONCLUSIONS

The results of the PPA of reaction (1) reported here are basically in agreement with those obtained for reaction (2). Difficulties for a direct comparison arise from the limited statistics: Only 5190 events are available for reaction (1) to be compared with nearly 25 000 for reaction (2) [1].

There is, however, some indication that the method itself is at the limits of its applicability: Processes which proceed via dynamical mechanisms which occupy distinct and different regions in phase-space, can be well separated; thus only small overlaps remain between the three classes which dominate reactions (1) and (2): pion diffraction dissociation (i.e. A meson production), Reggeon exchange, and proton diffraction dissociation. The resolution is still satisfactory inside the second class where double resonance production strongly reduces the available phase-space, which in turn reduces overlaps.

Inside the A meson and proton diffraction dissociation sample, however, no reliable cross sections can be obtained; the reason for this is not only the close neighbourhood in phase-space, but also the presence of strong interference effects. Nevertheless, the kinematic distributions of the PPA separated samples exhibit strong characteristics properties, which indicates that a certain, but incomplete, resolution has been achieved. The degree of residual overlap can be estimated calculating the overlap matrix OV_{ij} from the final weights after the procedure has converged.

On the other hand, the PPA is an effective means for "scanning" phase-space for hidden phenomena: Processes contributing to a certain final state, but not considered by the analyzing physicist, will - as far as they are not below the threshold of resolution - signal their presence in an advanced state of the procedure as they will show up in the control distributions. This happened in the analysis of reaction (2) and led to the introduction of the A'^{+}(1800)-state.

Here we present evidence for the existence of the corresponding negatively charged A'(1800). After a series of checks, we find it impossible to interpret the A' as due to reflexions from other channels. Not only has the A'^{-} survived the iteration procedure but it also exhibits the same characteristic decay angular distributions in either charge state. More information on the A' is expected from a Partial Wave Analysis.

We are indebted to the operation crews of the CERN 2m Bubble Chamber and the constructors of the beam. We would like to thank the scanning, measuring and computing staff at each of our laboratories.

RÉFERENCES

[1] M. Deutschmann et al., Aachen-Berlin-Bonn-CERN-Cracow-Heidelberg-Warsaw Collaboration, Nucl. Phys. B99 (1975) 397.

[2] J.E. Brau et al., Phys. Rev. Letters 27 (1971) 1481.

[3] M. Deutschmann et al., Aachen-Berlin-Bonn-CERN-Cracow-Heidelberg Collaboration, Nucl. Phys. B86 (1975) 221.

[4] G. Otter et al., Aachen-Berlin-Bonn-CERN-Heidelberg Collaboration, Nucl. Phys. B80 (1974).

TABLE CAPTIONS

Table 1 List of channels contributing to reaction (1) and numbers of events attributed after convergence of the PPA iteration procedure.

Table 2 Overlap matrix OV_{ij} indicating the percent overlap in phase-space between channels i and j.

Table 3 Overlap matrix for the three dominant processes (pion dissociation, Reggeon exchange and proton diffraction dissociation).

Table 4 Cross sections for reaction (1) and for reaction (2) as far as comparable.

CERN/EP/PHYS 76-41

TABLE 1

Reaction Channel	Number of Events Attributed
(1.1) $\pi^- p \to A_1^- p$, $A_1^- \to \rho^o \pi^-$	1 987
(1.2) $\to A_2^- p$, $A_2^- \to \rho^o \pi^-$	229
(1.3) $\to A_3^- p$, $A_3^- \to f \pi^-$	369
(1.4) $\to A'^- p$, $A'^- \to \rho^o \pi^-$.	258
(1.5) $\to (p\pi^-)\ \rho^o$	416
(1.6) $\to (p\pi^-)\ f$	139
(1.7) $\to \Delta^{++}(1236)\pi^-\pi^-$	204
(1.8) $\to \pi^-(p\pi^+\pi^-)_{DD}$	765
(1.9) $\to \pi^-(\Delta^{++}\pi^-)_{DD}$	676

TABLE 2

	A_1^-p	A_2^-p	A_3^-p	A'^-p	$(p\pi^-)\rho^o$	$(p\pi^-)f$	$\Delta^{++}\pi^-\pi^-$	$(p\pi^+\pi^-)_{DD}\pi^-$	$(\Delta^{++}\pi^-)_{DD}\pi^-$
A_1^-p	-	9	9	6	5	1	1	1	1
A_2^-p	40	-	9	6	10	1	1	0	1
A_3^-p	32	8	-	17	9	4	2	1	3
A'^-p	24	6	19	-	15	6	5	5	9
$(p\pi^-)\rho^o$	16	8	8	12	-	9	0	6	4
$(p\pi^-)f$	7	2	10	12	21	-	1	18	13
$\Delta^{++}\pi^-\pi^-$	6	1	4	8	1	1	-	12	23
$(p\pi^+\pi^-)_{DD}\pi^-$	1	0	1	3	4	5	4	-	25
$(\Delta^{++}\pi^-)_{DD}\pi^-$	3	0	2	5	3	4	7	26	-

TABLE 3

	Channels 1-4	Channels 5-7	Channels 8-9
Channels 1-4	-	7	3
Channels 5-7	19	-	13
Channels 8-9	5	10	-

TABLE 4

Reaction Channel	Cross Section (μb)	Reaction Channel	Cross Section (μb)
$\pi^- p \to (A_1^- + A_2^- + A'^-)p$	539 ± 32	$\pi^+ p \to (A_1^+ + A_2^+ + A'^+)p$	519 ± 27
$\to A_3^- p$	80 ± 14	$\to A_3^+ p$	71 ± 11
$\to (\text{all } A^-)p$	619 ± 40	$\to (\text{all } A^+)p$	590 ± 29
$\to (p\pi^-)\rho^o$	91 ± 15		
$\to (p\pi^-)f$	30 ± 9		
$\to \Delta^{++}(1236)\pi^-\pi^-$	44 ± 10		
$\to \pi^-(p\pi^+\pi^-)_{DD}$	312 ± 27	$\to \pi^+(p\pi^+\pi^-)_{DD}$	266 ± 19

FIGURE CAPTIONS

Fig. 1 Effective mass distributions of various two- and three-particle systems for the total sample of 5190 events of the reaction $\pi^- p \to p\pi^+\pi^-\pi^-$ at 16 GeV/c.

Fig. 2 Effective mass distributions of the (3π) and $(\pi^+\pi^-)$ systems for the sum of the two channels (1.1 and 1.2): $\pi^- p \to A_1^- p$ and $\pi^- p \to A_2^- p$, with A_1^- and A_2^- decaying into $\rho^o\pi^-$.

Fig. 3 Effective mass, momentum transfer and decay angular distributions for the channel (1.3): $\pi^- p \to A_3^- p$, with $A_3^- \to f\pi$.

Fig. 4 Effective mass, momentum transfer and decay angular distributions for the channel (1.4): $\pi^- p \to A'^- p$, with $A'^- \to \rho^o\pi^-$.

Fig. 5 Effective mass, momentum transfer and decay angular distributions for the channel (1.5): $\pi^- p \to (p\pi^-)\ \rho^o$.

Fig. 6 Effective mass, momentum transfer and decay angular distributions for the channel (1.6): $\pi^- p \to (p\pi^-)\ f$.

Fig. 7 Effective mass, momentum transfer and decay angular distributions for the channel (1.7): $\pi^- p \to \Delta^{++}(1236)\ \pi^-\pi^-$.

Fig. 8 Effective mass, momentum transfer and decay angular distributions for the channel (1.8): $\pi^- p \to (p\pi^+\pi^-)_{DD}\ \pi^-$.

Fig. 9 Effective mass, momentum transfer and decay angular distributions for the channel (1.9): $\pi^- p \to (\Delta^{++}\pi^-)_{DD}\ \pi^-$.

Fig. 10 Effective mass distributions for the untagged events.

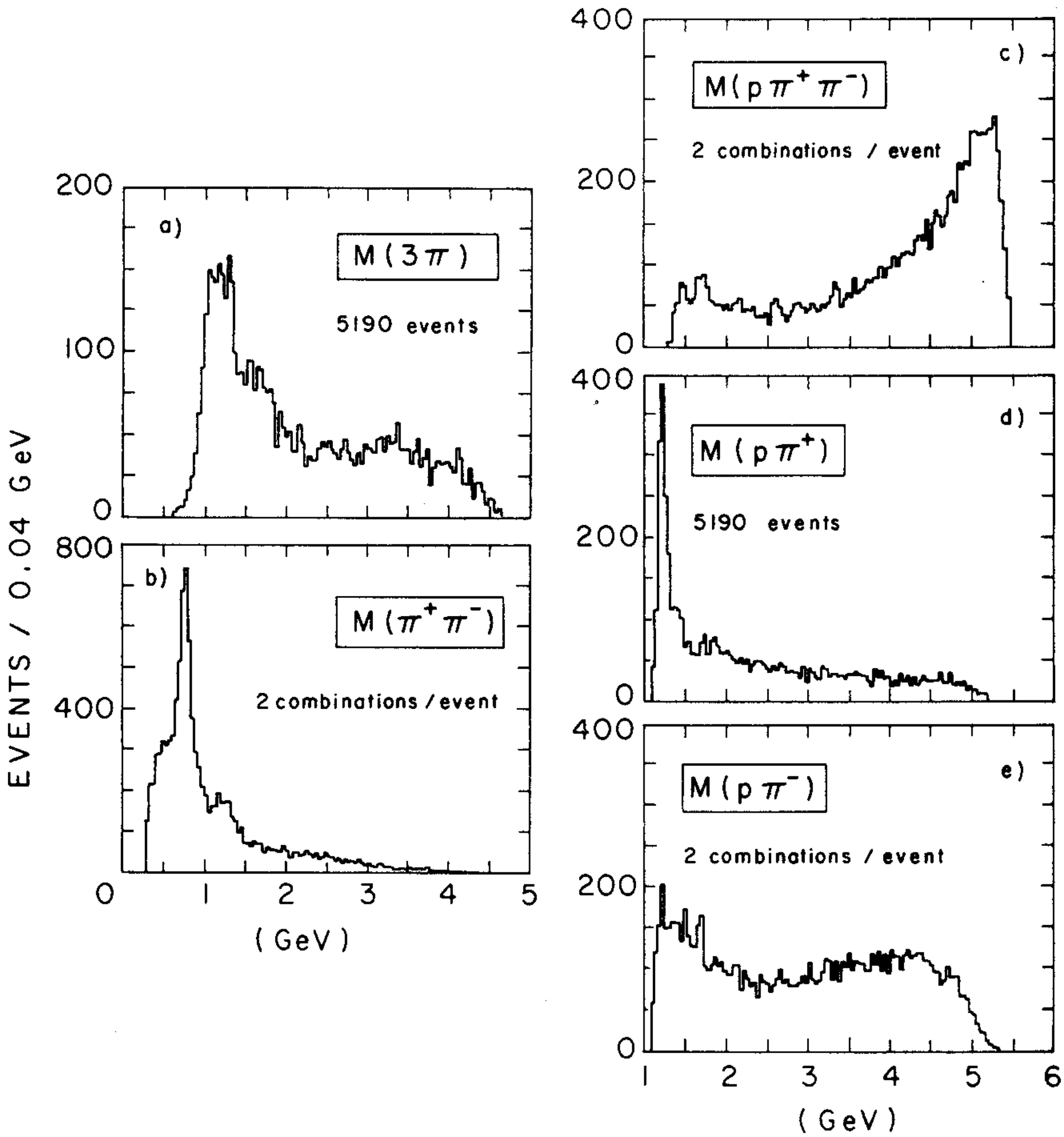

EVENTS / 0.04 GeV
a)
M(3π)
5190 events
b)
M(π⁺π⁻)
2 combinations / event
(GeV)
c)
M(pπ⁺π⁻)
2 combinations / event
d)
M(pπ⁺)
5190 events
e)
M(pπ⁻)
2 combinations / event
(GeV)

Fig. 1

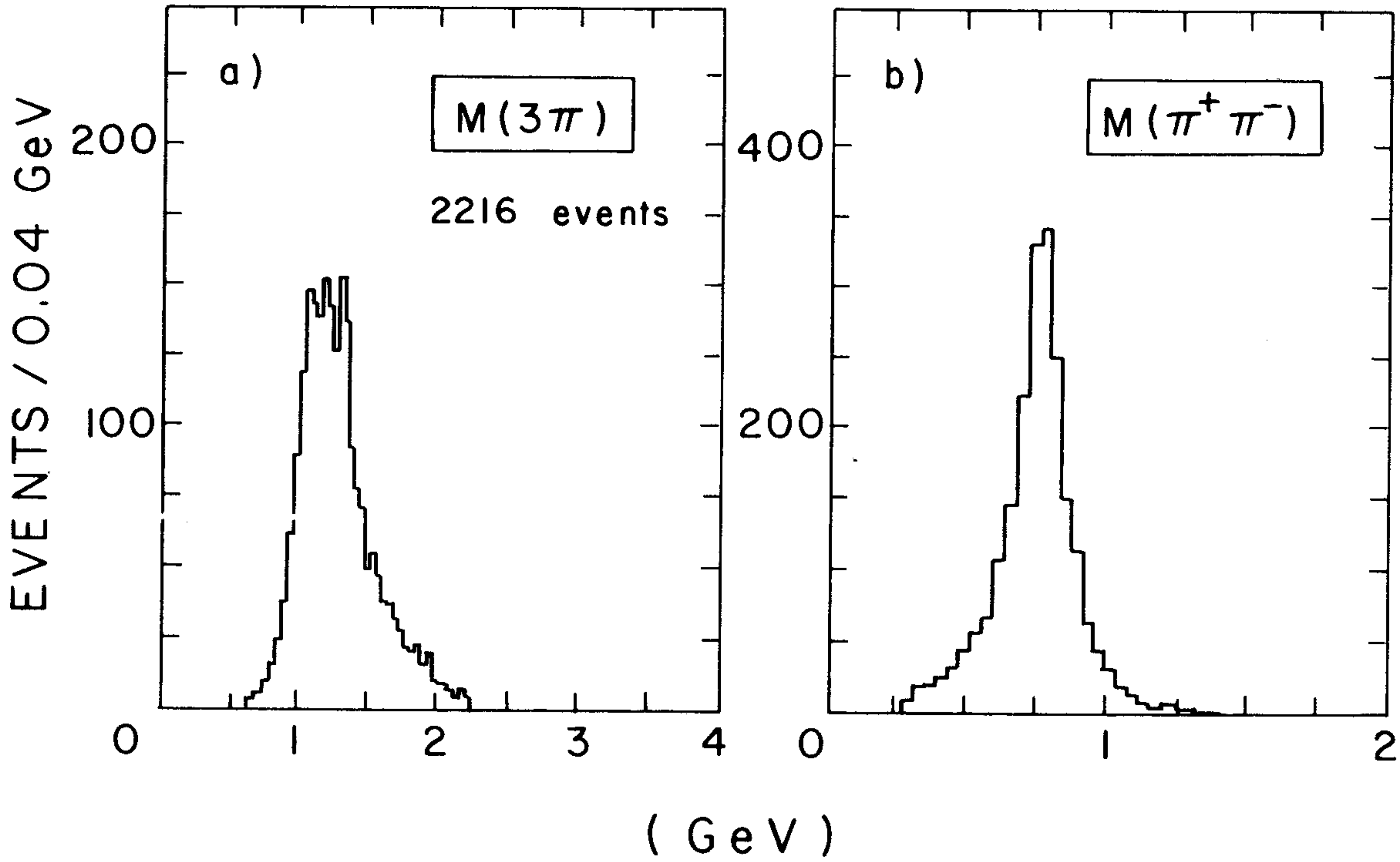
EVENTS / 0.04 GeV
a)
M(3π)
2216 events
b)
M(π⁺π⁻)
200
100
0
400
200
0
1
2
3
4
1
2
(GeV)

Fig. 2

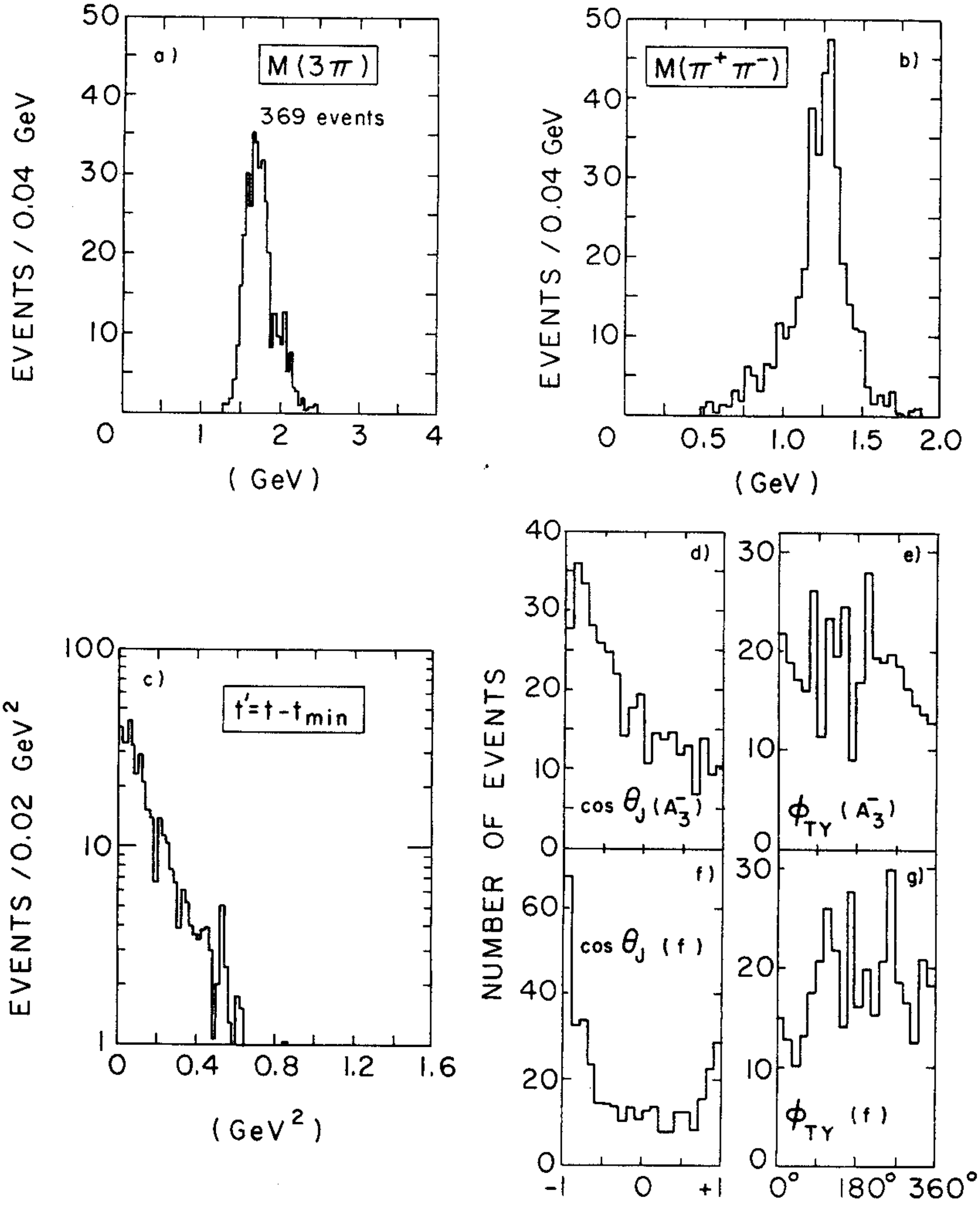

a)
M(3π)
369 events
EVENTS / 0.04 GeV
(GeV)
b)
M(π⁺π⁻)
EVENTS / 0.04 GeV
(GeV)
c)
t′=t-t_min
EVENTS /0.02 GeV²
(GeV²)
d)
cos θ_J (A₃⁻)
e)
φ_TY (A₃⁻)
f)
cos θ_J (f)
g)
φ_TY (f)
NUMBER OF EVENTS

Fig. 3

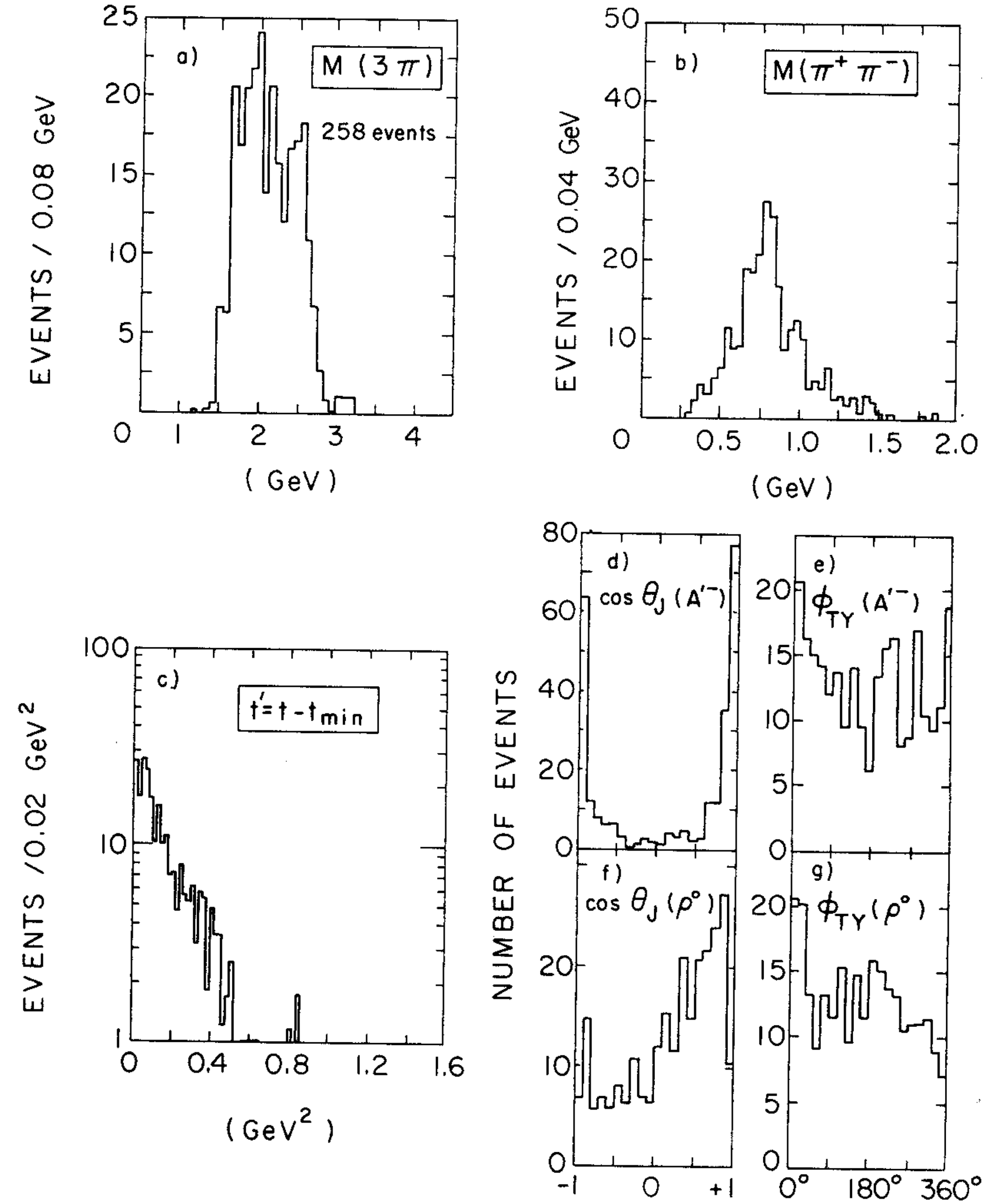
a)
M (3π)
258 events
EVENTS / 0.08 GeV
(GeV)
b)
M(π⁺π⁻)
EVENTS / 0.04 GeV
(GeV)
c)
t'=t-tmin
EVENTS /0.02 GeV²
(GeV²)
d)
cos θJ (A'⁻)
e)
φTY (A'⁻)
f)
cos θJ (ρ°)
g)
φTY (ρ°)
NUMBER OF EVENTS

Fig. 4

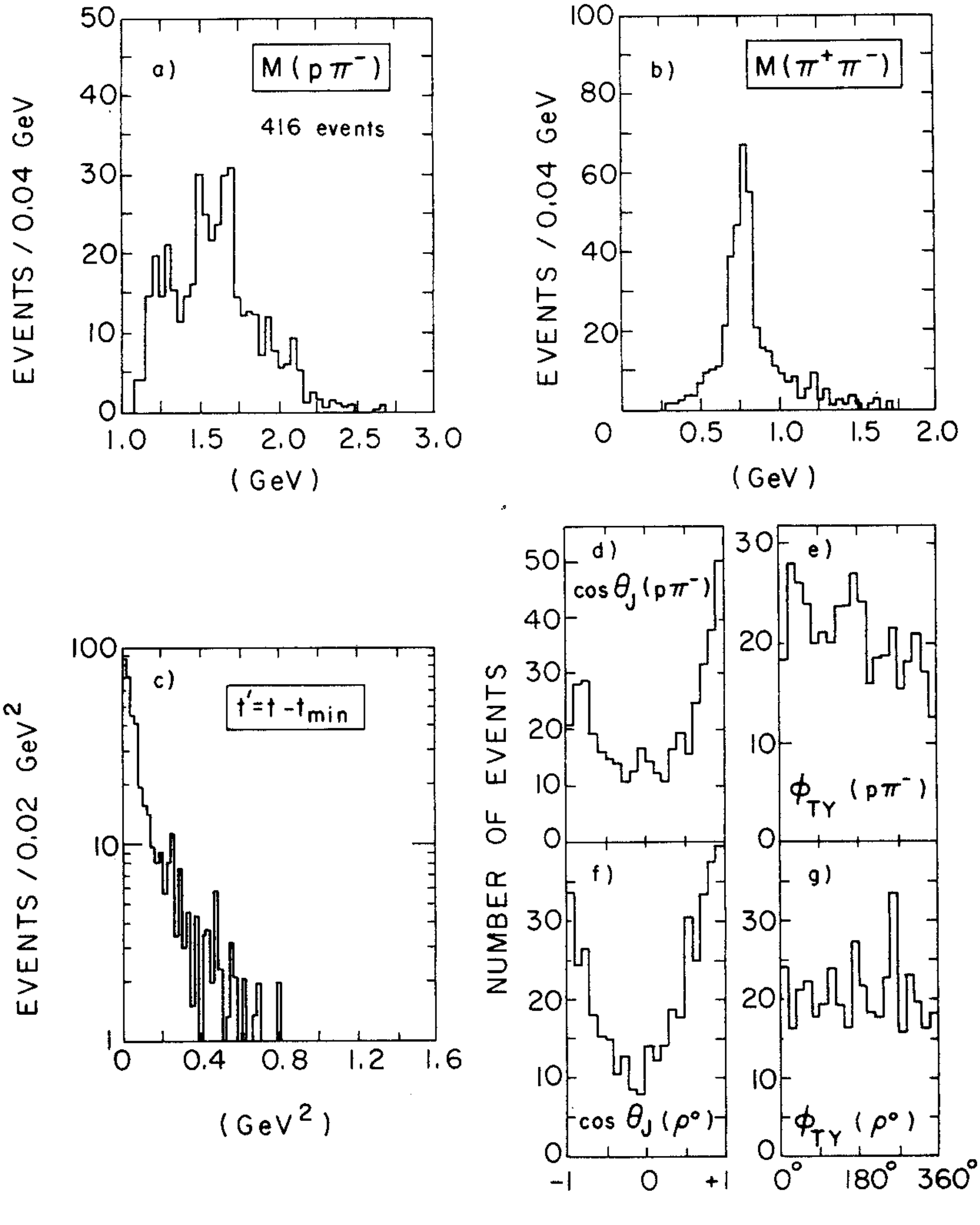

a)
M(pπ⁻)
416 events
EVENTS / 0.04 GeV
(GeV)
b)
M(π⁺π⁻)
EVENTS / 0.04 GeV
(GeV)
c)
t′=t -tmin
EVENTS / 0.02 GeV²
(GeV²)
d)
cos θJ (pπ⁻)
e)
φTY (pπ⁻)
f)
cos θJ (ρ°)
g)
φTY (ρ°)
NUMBER OF EVENTS

Fig. 5

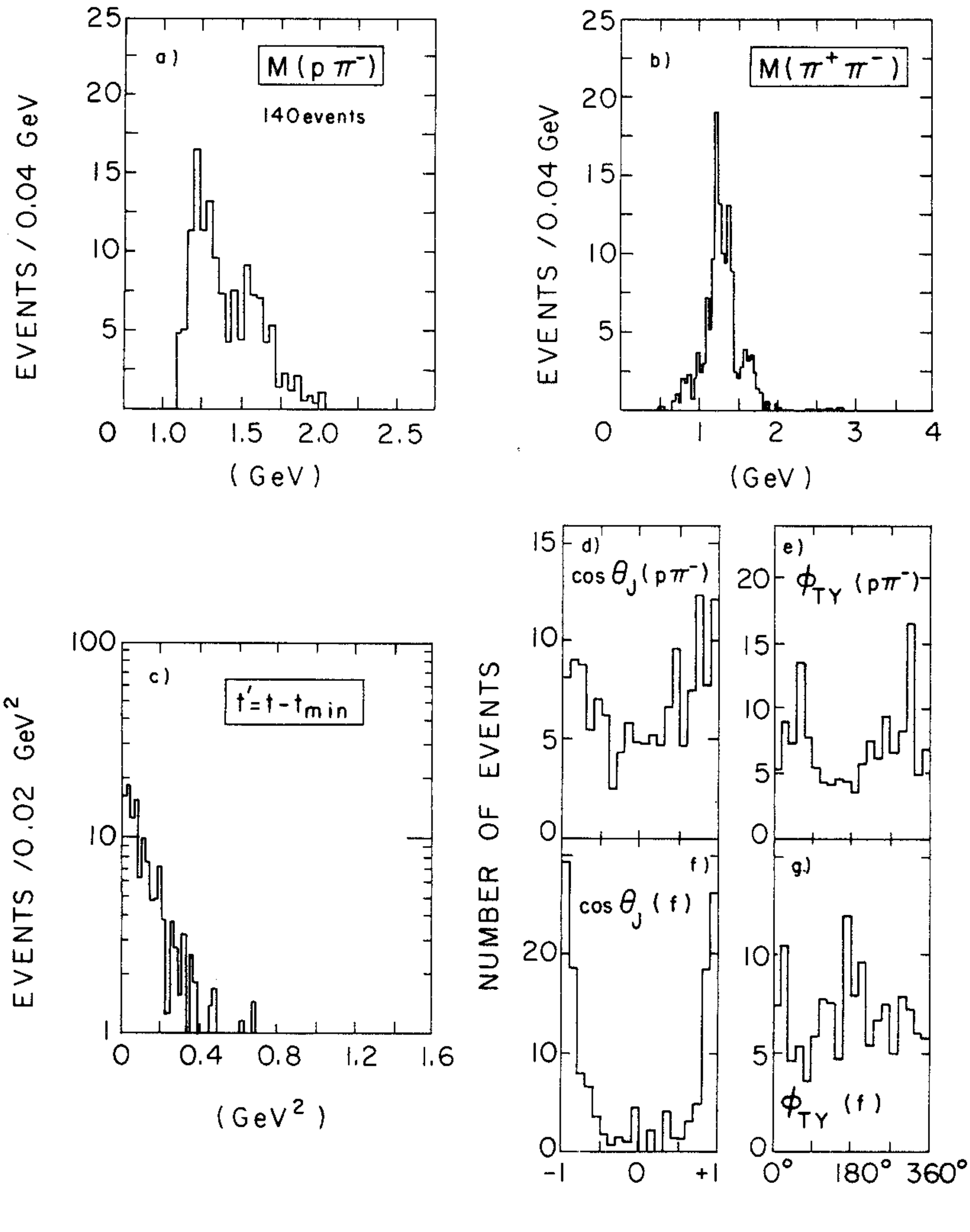

a)
M(p π⁻)
140 events
EVENTS / 0.04 GeV
(GeV)
b)
M(π⁺π⁻)
EVENTS /0.04 GeV
(GeV)
c)
t′=t-t_min
EVENTS /0.02 GeV²
(GeV²)
d)
cos θ_J (pπ⁻)
e)
φ_TY (pπ⁻)
f)
cos θ_J (f)
g)
φ_TY (f)
NUMBER OF EVENTS

Fig. 6

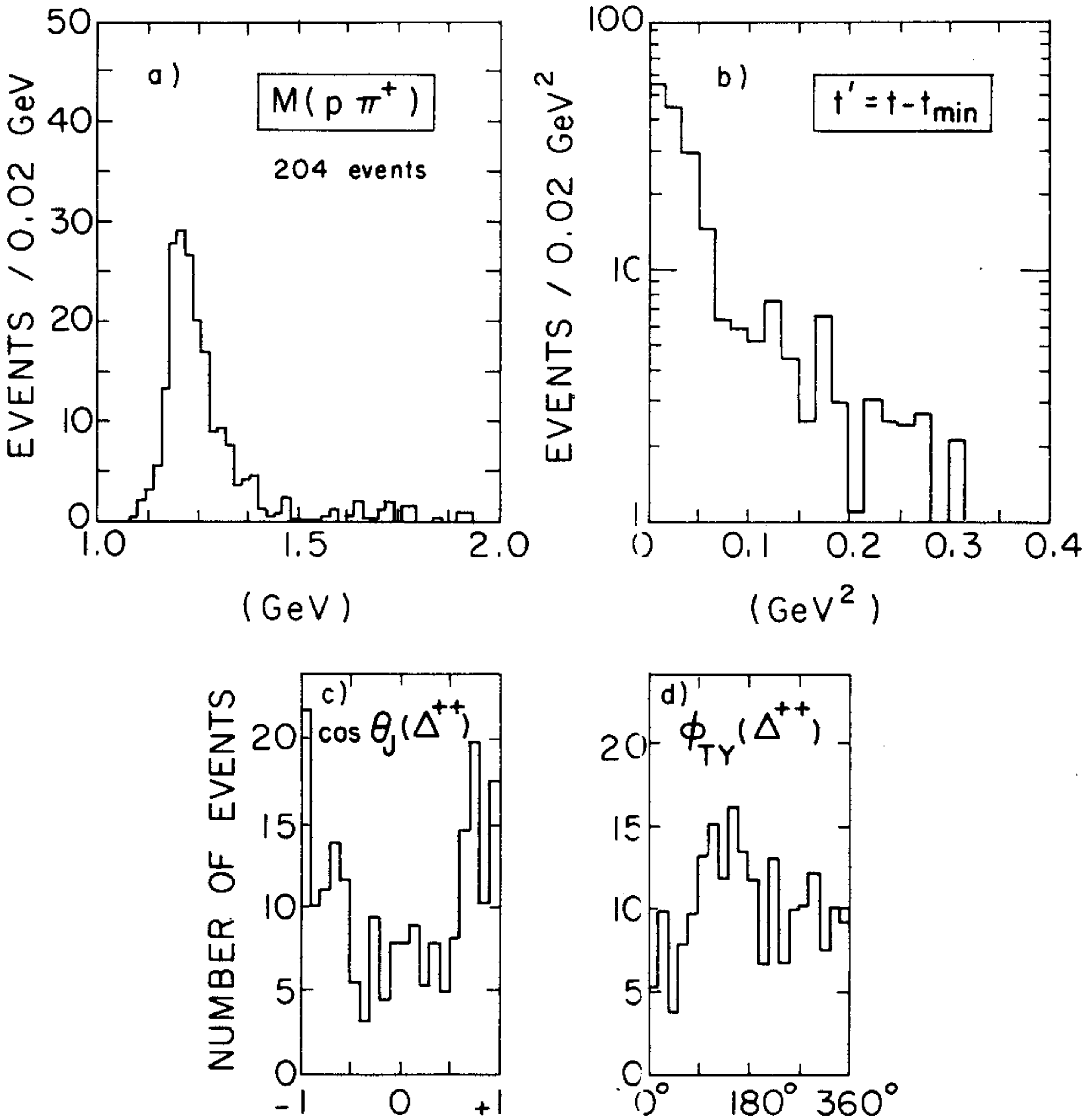

a)
M(p π+)
204 events
EVENTS / 0.02 GeV
(GeV)
b)
t' = t - tmin
EVENTS / 0.02 GeV2
(GeV2)
c)
cos θJ(Δ++)
NUMBER OF EVENTS
d)
φTY(Δ++)

Fig. 7

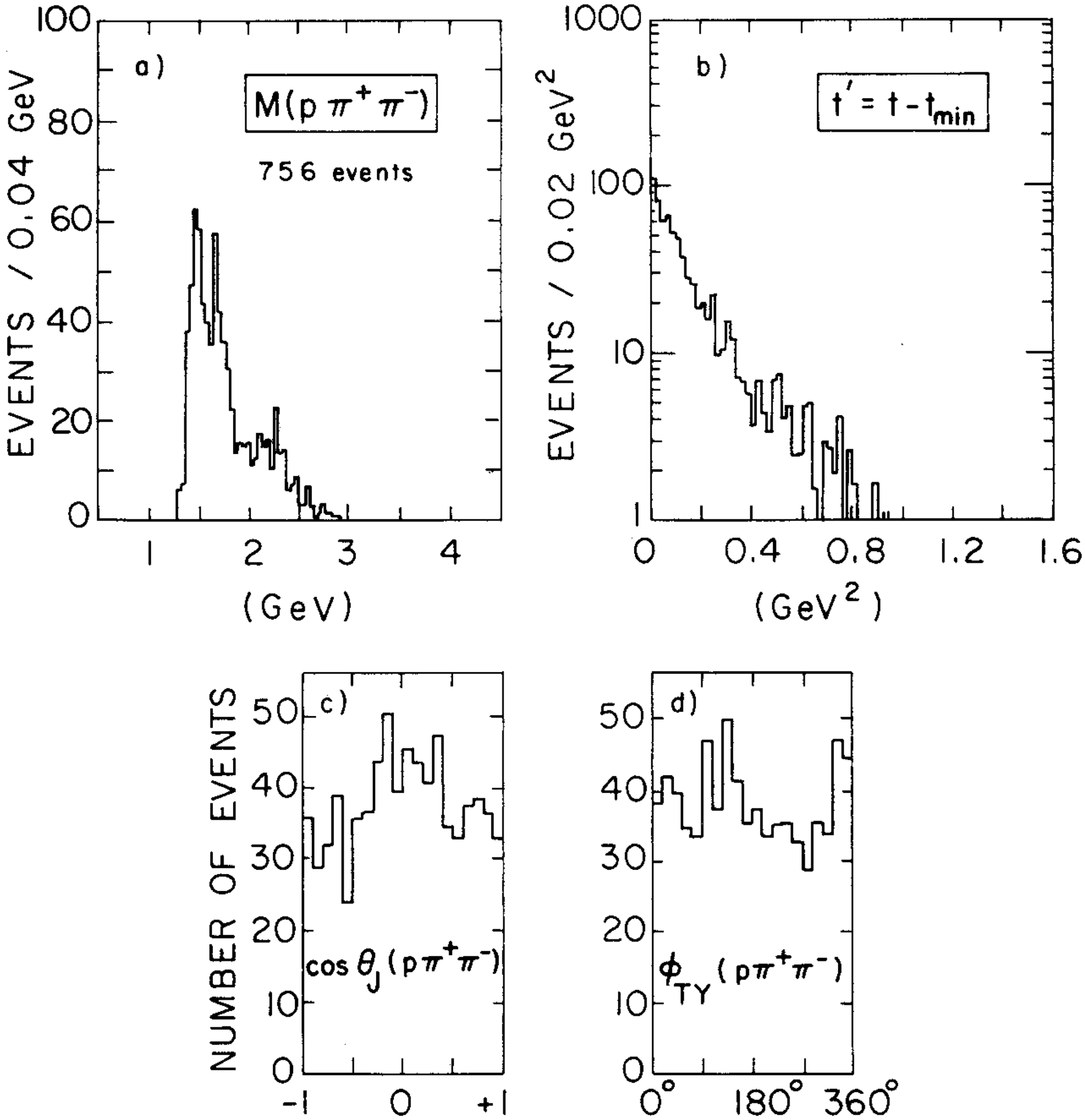

a)
M(pπ⁺π⁻)
756 events
EVENTS / 0.04 GeV
(GeV)
b)
t' = t - t_min
EVENTS / 0.02 GeV²
(GeV²)
c)
cos θ_J (pπ⁺π⁻)
NUMBER OF EVENTS
d)
φ_TY (pπ⁺π⁻)

Fig. 8

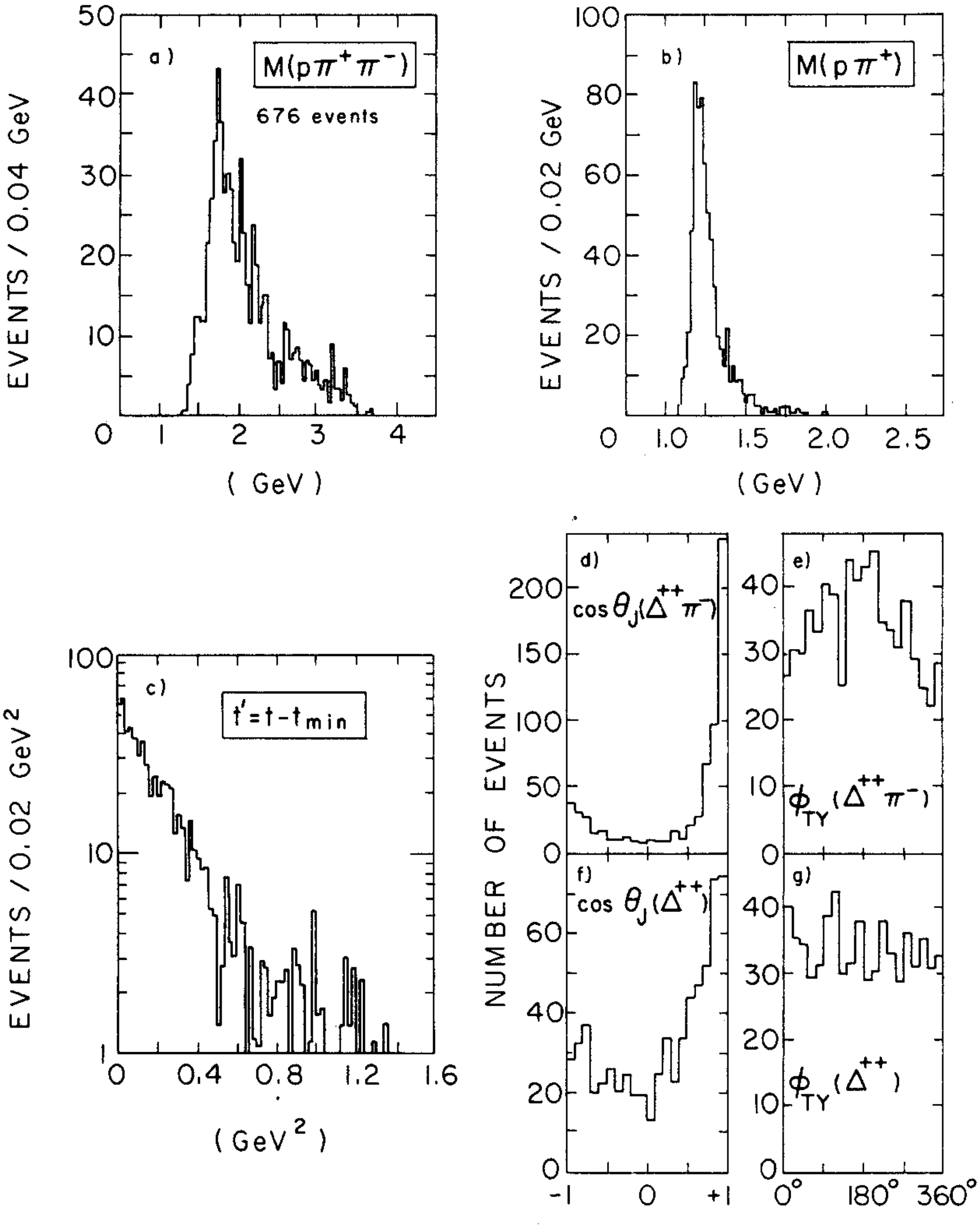

a)
M(pπ⁺π⁻)
676 events
EVENTS / 0.04 GeV
(GeV)
b)
M(pπ⁺)
EVENTS / 0.02 GeV
(GeV)
c)
t′=t-t min
EVENTS / 0.02 GeV²
(GeV²)
d)
cos θJ(Δ⁺⁺π⁻)
e)
φTY(Δ⁺⁺π⁻)
f)
cos θJ(Δ⁺⁺)
g)
φTY(Δ⁺⁺)
NUMBER OF EVENTS

Fig. 9

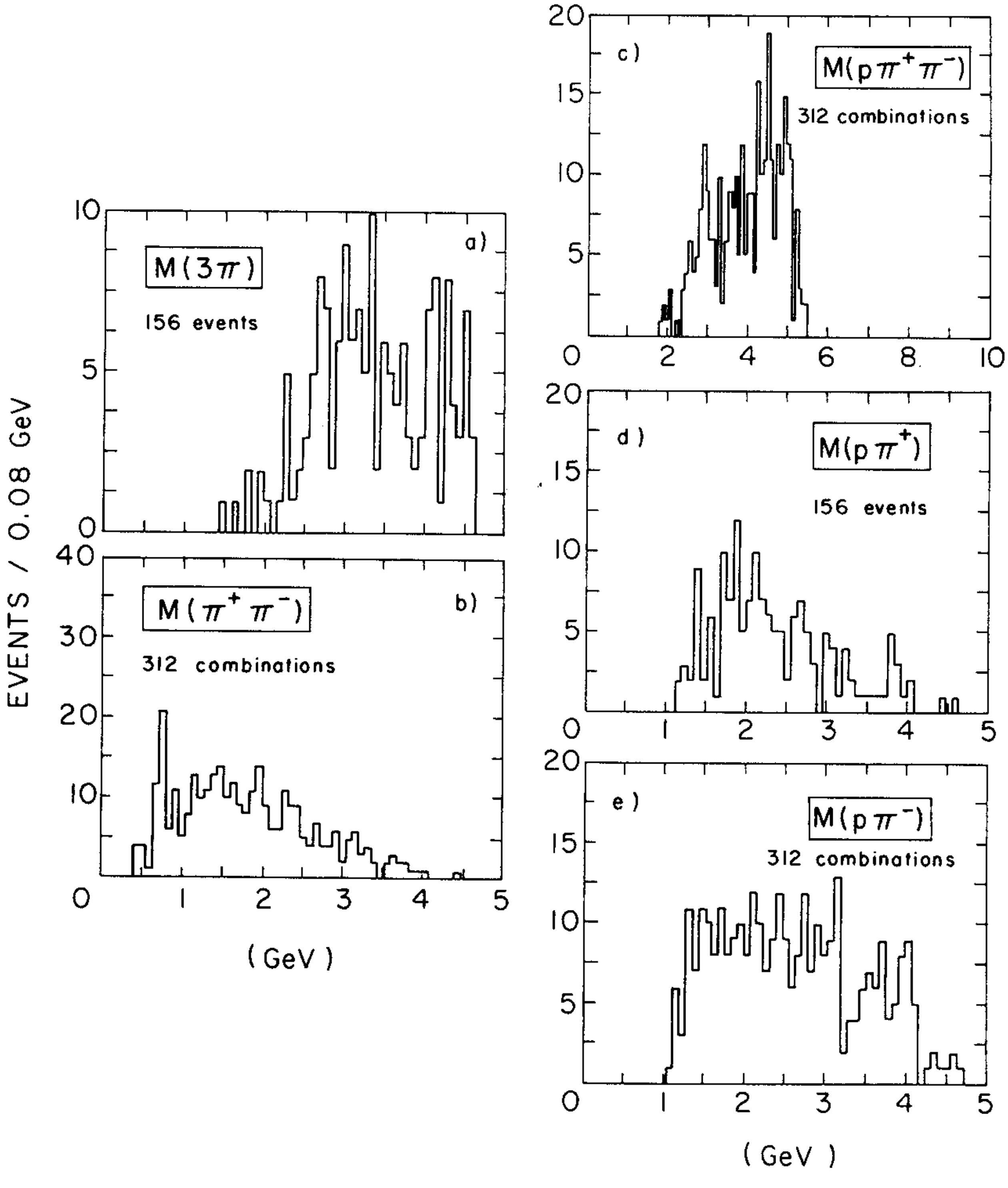

EVENTS / 0.08 GeV
M(3π)
156 events
a)
M(π⁺π⁻)
312 combinations
b)
(GeV)
c)
M(pπ⁺π⁻)
312 combinations
d)
M(pπ⁺)
156 events
e)
M(pπ⁻)
312 combinations
(GeV)

Fig. 10